

Received December 31, 2020; reviewed; accepted March 02, 2021

## Experimental and kinetic study of zinc leaching from metallurgical slag by 5-sulfosalicylic acid

Long Wang<sup>1</sup>, Hanyu Gao<sup>1</sup>, Shimin Song<sup>1</sup>, Na Xue<sup>1</sup>, Jinxia Zhang<sup>1</sup>, Siyuan Yang<sup>2,3</sup>, Cheng Liu<sup>3</sup>

<sup>1</sup> College of Mining Engineering, North China University of Science and Technology, Tangshan 063210, China

<sup>2</sup> Hubei Key Laboratory for Efficient Utilization and Agglomeration of Metallurgic Minerals Resources, Wuhan, 430081, China

<sup>3</sup> School of Resources and Environmental Engineering, Wuhan University of Technology, Wuhan, 430070, China

Corresponding authors: [siyuan.yang@whut.edu.cn](mailto:siyuan.yang@whut.edu.cn) (Siyuan Yang), [145601011@csu.edu.cn](mailto:145601011@csu.edu.cn) (Cheng Liu)

**Abstract:** As an organic acid with the characters of low corrosivity and extensive source, 5-sulfosalicylic acid (5-SSA) was firstly utilized as a potential leaching reagent for the recovery of zinc from metallurgical slag. Effects of stirring speed, leaching temperature, 5-SSA concentrations and size fraction on the leaching zinc leaching rate were investigated. A zinc leaching efficiency of 94.2% was achieved under the appropriate operating conditions (450 rpm of stirring speed, 50 °C of leaching temperature, 0.3 mol/L of 5-SSA concentration and d<sub>90</sub>=65 μm of size fraction), indicating that 5-SSA was an excellent leaching reagent of zinc oxide. SEM-EDS and specific surface aperture analyzer further reveal the well-developed micropores and cracks from zinc metallurgical slag, which could be assigned to the removal of zinc oxide encapsulated in the sample. In addition, the leaching kinetics of zinc metallurgical slag in the 5-SSA was studied. It was found that the surface chemical reaction model satisfactorily predicted the zinc leaching rate. A reaction kinetic equation was finally established for the zinc leaching rate.

**Keywords:** zinc metallurgical slag, 5-sulfosalicylic acid, leaching kinetics, resource recovery

### 1. Introduction

Zinc is one of the most important metals used for various industrial, medical, chemical and high-technology applications today (Liu et al., 2018; Yang et al., 2016a). Sphalerite is the chief ore mineral of zinc. Zinc ore is also found as smithsonite, zincite, hemimorphite, willemite and zinc ferrite (Li et al., 2015; Mahedi et al., 2019). As is well-known, sphalerite is naturally hydrophobic and could thus be easily recovered by flotation (Zhang et al., 2016b). However, as Zn production rate keeps growing in response to increasing market demand, high-grade and easy-floated deposits become depleted (Güler and Seyrankaya, 2016; Seyed Ghasemi and Azizi, 2018). As a consequence, Zn mines of the future will be lower grade and more complex operations.

Waste reprocessing of zinc oxide ore and other zinc oxide resources hence becomes a vital alternative to recover zinc. Metallurgical slag, the by-product of the metallurgical industry, is an important zinc oxide source and has attracted lots of research interest in zinc recovery (Asadi et al., 2017; Chairaksa-Fujimoto et al., 2016). Unlike zinc sulfide ore, zinc oxide is usually hydrophilic, which means the separation is not easily achieved through physical separation methods, but hydrometallurgy is an efficient method to extract zinc from metallurgical slag (Behnajady and Moghaddam, 2017; Ehsani and Obut, 2019).

Zinc oxide slag is commonly leached in the inorganic acid or alkaline solution, such as sulfide acid, sodium hydroxide and ammonium salt (Rao et al., 2015; Şahin and Erdem, 2015). Once the appropriate leaching reagent was selected, zinc oxide is dissolved as Zn<sup>2+</sup> in the solution, and normally recovered

by the extraction and electrodeposition (Gu et al., 2019). Inorganic acid (e.g., sulfuric acid) and alkaline (e.g., sodium hydroxide) leaching reagents usually erode the leaching equipment and cause environmental problems (Zhang et al., 2016a). Due to their relatively low corrosivity, organic acids became widely used as the leaching reagent to extract zinc from zinc oxide (Irannajad; et al., 2013; Ru et al., 2015; Yang et al., 2016b). Most researches have been conducted on the zinc recovery from metallurgical slag through a single chemical reaction (neutral reaction or complexation reaction). In contrast, zinc recovery by organic acid through multiple chemical reactions is rarely reported up to the present.

5-sulfosalicylic acid (5-SSA) is a commonly used raw or intermediate material in the manufacture of dye, surfactant, and medicine (Xiao et al., 2016; Xu et al., 2019). The carboxyl group and sulfonic acid group in 5-SSA can be ionized in an aqueous solution and present strong affinity with metal ions (Wang et al., 2017; Xu et al., 2019). The combination of neutral reaction (zinc oxide with  $H^+$ ) and complexation reaction ( $Zn^{2+}$  with carboxyl group), making 5-SSA a potentially cheap and efficient leaching reagent for the extraction of zinc from metallurgical slag (Jin et al., 2019; Lin et al., 2018).

In the present study, 5-SSA was firstly utilized in the leaching of zinc metallurgical slag. The leaching parameters such as stirring speed, temperature, reagent concentration, and particle size were investigated to obtain the optimal conditions. The zinc oxide slag before and after leaching was characterized to reveal the leaching mechanism of 5-SSA. Furthermore, the leaching kinetics was studied through the shrinking core model, and the kinetic model was subsequently established to determine the reaction control steps. The research guides 5-SSA application not only in the zinc recovery from zinc oxide slag but also in the leaching of other metal oxides.

## 2. Materials and methods

### 2.1. Materials and reagents

The metallurgical slag used in this study was obtained from Tangshan Iron & Steel Company, Hebei Province, China. The samples were crushed to the desired size fractions using a jaw crusher and ball grinder. X-ray diffraction (XRD) analysis of the metallurgical slag was conducted and shown in Fig. 1, indicating the main components of samples are spartalite, hematite and quartz. The chemical composition of the metallurgical slag (Table 1) confirmed that the zinc content of the studied metallurgical slag is 22.62%.

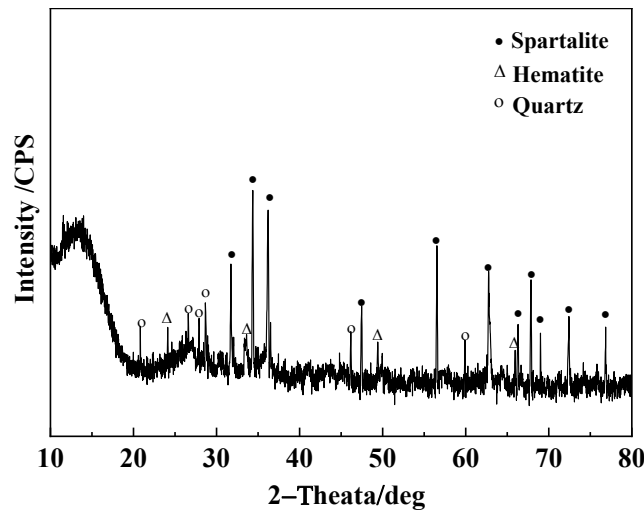


Fig. 1. XRD pattern of the metallurgical slag

Table 1. Chemical composition of the metallurgical slag (wt%)

Component	TFe	Zn	MgO	SiO <sub>2</sub>	CaO	Al <sub>2</sub> O <sub>3</sub>	Ignition Loss
Content	34.65	22.62	2.03	14.16	4.41	1.54	20.59

The chemically pure reagent (5-SSA) is purchased from Dingshenxin Chemical Engineering Co., Ltd. in Tianjin, China, the molecular structure of 5-SSA is shown in Fig. 2. Deionized water with a resistance of 18.2 M $\Omega$ ·cm was employed for all experiments, as it can eliminate the adverse effects of water impurities (Liu et al, 2021).

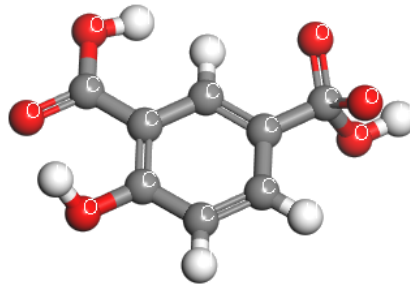


Fig. 2. Molecular structure of 5-SSA

## 2.2. Leaching experiments

Fig. 3 presents the diagram of setup for the leaching of metallurgical slag containing zinc oxide that has been widely used in leaching experiments (Wang et al., 2020a). Specifically, it consists of a water bath with a magnetic stirrer, reaction flask and condenser pipe. In each experiment, a 200 mL 5-SSA solution with required concentration was put in the sealed flask and heated to a certain temperature. Then 2 g of zinc metallurgical slag with different size fractions were added into the flask, wherein the effects of temperature, stirring rate, reagent concentration and particle size on leaching efficiency was investigated. Note that  $d_{90}$  (particle diameter at 90% in the cumulative distribution) was chosen to present the size fractions of samples in this study. During the experiment, 2 mL leachate was taken out at specific time intervals and analyzed by inductively coupled plasma atomic emission spectroscopy (ICP-AES, ULTIMA2, HORIBA Jobin Yvon). Based on the zinc content of leachate in a timeline, the leaching rate (%) of zinc from metallurgical slag can be calculated. The zinc leaching rate was the percentage of zinc leached. The zinc leaching rate was calculated as follows:

$$\varphi_i = \frac{(V_0 - \sum_{i=1}^{i-1} V_i) C_i + \sum_{i=1}^{i-1} V_i C_i}{M\beta} \quad (1)$$

where  $\varphi_i$  is the zinc leaching rate (%) for the sample  $i$  at specific time intervals,  $V_0$  is the initial volume (L),  $V_i$  is the volume (L) of leachate taken for analyzation for sample  $i$ ,  $C_i$  is the concentration (g/L) of zinc in the leachate for the sample  $i$ ,  $M$  is the mass (g) of metallurgical slag added into the flask,  $\beta$  is the grade (%) of the metallurgical slag.

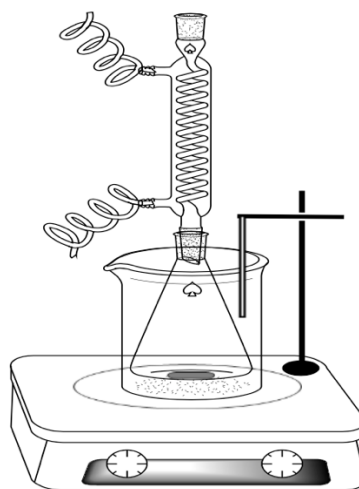
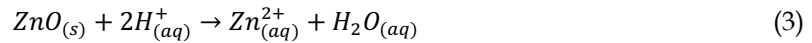
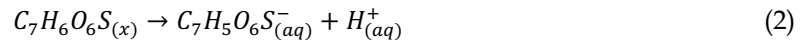


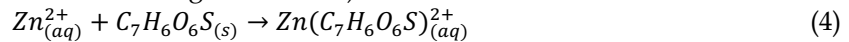
Fig. 3. Schematic diagram of the leaching equipment

### 2.3. Reaction mechanism

The hydroxyl, carboxyl and sulfonic group in 5-SSA can be hydrolyzed in an aqueous solution, causing the chemical reaction between zinc oxide and  $H^+$ , which can be summarized as the neutral reaction by following equations (Bryndal et al., 2014; Cao et al., 2016; Chen et al., 2014).



In addition, metallic ions can easily react with the anion group and form a stable chelate complex. Some researchers found that metal ions in aqueous solutions (e.g.  $Al^{3+}$ ,  $Cu^{2+}$ ,  $Zn^{2+}$ ,  $Fe^{3+}$ ,  $Ni^{2+}$ ) can form stable complexes with certain organic substances containing amino, carboxyl, hydroxyl and other groups (Falagán et al., 2017; Li et al., 2020; Wang et al., 2020b).



Therefore, the neutral reaction and the complexation reaction dominant the 5-SSA as leaching reagent in the zinc recovery metallurgical slag.

### 2.4. Scanning electron microscopy

Before and after leaching, the zinc metallurgical slag was filtered, washed and dried in an oven at 40°C. They were platinum coated in a sputter coater for preparing samples, more details can be found in the references (Yang et al., 2017). A scanning electron microscope (SEM, Philips XL30ESEM-TMP) under an accelerating voltage of 10 kV was conducted to investigate the morphology of these samples. Meanwhile, the element mappings of studied samples were also conducted by energy dispersive spectroscopy (EDS).

### 2.5. Structure analysis

The samples before and after extraction were prepared under the required leaching conditions. The 1.0000 g of zinc metallurgical slag was initially heated under the vacuum oven to remove the air and moisture. The nitrogen was then given to the test tube under the required pressure and removed subsequently to evaluate the specific surface area and micropore structure using the specific surface aperture analyzer (JW-BK112).

## 3. Results and discussion

### 3.1. Effects of stirring speed on the leaching efficiency of zinc metallurgical slag

Fig. 4 presents the influences of stirring speed on the zinc leaching rate. It is obvious that the leaching efficiency of zinc metallurgical slag increased with increasing stirring speed, which can be attributed to the better mixture and contact of samples with 5-SSA. Specifically, the zinc leaching rate enhanced markedly from 78.1% to 90.2% when the stirring speed was improved from 150 rpm to 450 rpm. Note that when the stirring rate further increased to 600 rpm, the zinc leaching rate exhibited only 1.2% improvement. Therefore, the stirring rate of 450 rpm was adopted in the subsequent leaching experiments.

### 3.2. Effects of leaching temperature on the leaching efficiency of zinc metallurgical slag

To investigate the effects of leaching temperature on zinc leaching rate, five different leaching temperatures ranged from 30 to 70 °C were tested. Fig. 5 shows that the leaching temperature significantly affects zinc leaching rate, in which the zinc leaching rate increased with increasing leaching temperature. Almost 95% zinc was digested within 24 min when the leaching temperature was 70 °C, wherein the zinc leaching rate was 80.2%, 51.2%, 41.2% and 20.6% when leaching temperature was 60 °C, 50 °C, 40 °C, 30 °C, respectively. It is also worth noting that the zinc leaching rate further enhanced with the time extension, and the final maximum values were 91.3% at 60 °C, 90.2% at 50 °C, 74.5% at 40 °C and 50.1% at 30 °C, separately. In addition, the enhancement of leaching temperature is devoted to the decline of solution viscosity and improvement of diffusion and mass transfer efficiency. Thus, the increase of the leaching temperature shortened the reaction time and boosted the leaching rate.

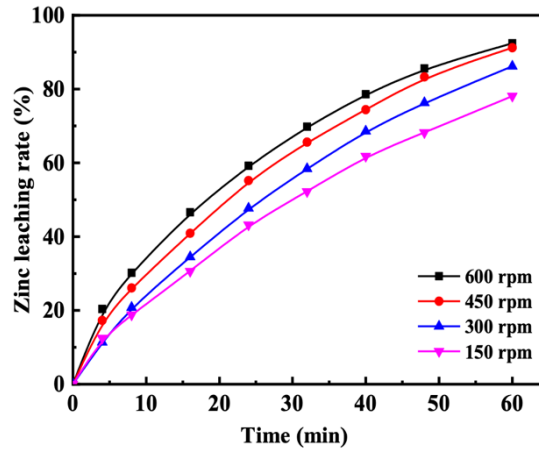


Fig. 4. Effect of stirring speed on the zinc leaching rate (temperature: 50 °C, 5-SSA concentration: 0.3 mol/L, size:  $d_{90}=65\ \mu\text{m}$ )

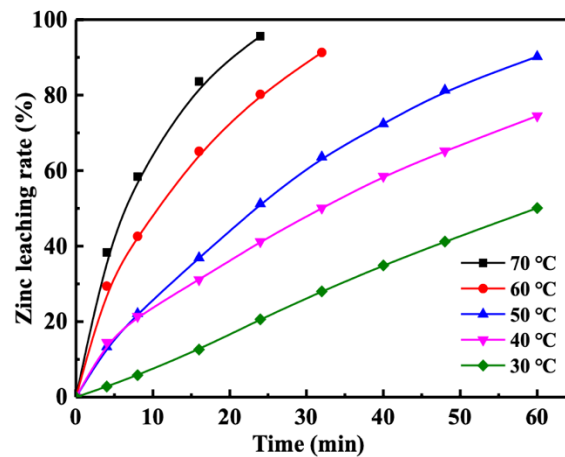


Fig. 5. Effect of leaching temperature on the zinc leaching rate (stirring speed: 450 rpm, 5-SSA concentration: 0.3 mol/L, size:  $d_{90}=65\ \mu\text{m}$ )

### 3.3. Effects of 5-SSA concentration on the leaching efficiency of zinc metallurgical slag

It is all known that the concentration of leaching reagent determines the leaching rate. The role of 5-SSA concentration ranging from 0.1 to 0.6 mol/L on zinc leaching efficiency was studied, the results of which were shown in Fig. 6. It reveals that zinc leaching rate increased with enhancing the 5-SSA concentration. After 60 min, zinc leaching efficiency at 0.6 mol/L 5-SSA was nearly 97%, whereas the leaching rate of zinc decreased dramatically to 76.2% at 0.1 mol/L 5-SSA. The increase of 5-SSA concentration improved the reaction efficiency between zinc oxide and leaching reagent, thereby the improvement of 5-SSA concentration had a positive effect on zinc extraction rate.

### 3.4. Effect of size fractions on the leaching efficiency of zinc metallurgical slag

The influences of size fractions of zinc metallurgical slag on the zinc leaching rate were also examined, considering the studied samples had a wide range of size distributions. Five typical size fractions were chosen as the variate, the results of which were shown in Fig. 7. As can be seen from it, the zinc leaching rate exhibits an opposite trend with particle size. Specifically, zinc leaching rate was the highest (94.2%) with  $d_{90}$  of 47  $\mu\text{m}$ , while it declined to 90.2%, 83.3%, 71.1% and 53.8% when the  $d_{90}$  increased to 65, 86, 132 and 286  $\mu\text{m}$ . With the decrease of particle size, more zinc oxide is liberated from the cover of metallurgical slag, leading to the remarkable enhancement of the contact and collision possibility between 5-SSA and zinc oxide. In addition, the decrease of particle size facilitates the diffusion of  $\text{H}^+$  and  $\text{Zn}(\text{C}_7\text{H}_6\text{O}_6\text{S})^{2+}$ , which can significantly accelerate the reaction speed.

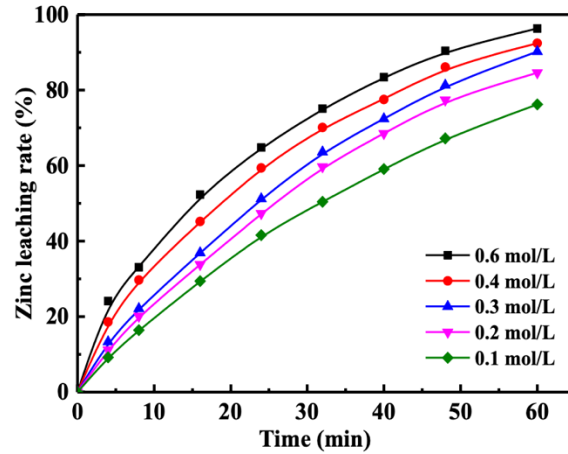


Fig. 6. Effects of 5-SSA concentration on the zinc leaching rate (stirring speed: 450 rpm, temperature: 50 °C, size:  $d_{90}=65\ \mu\text{m}$ )

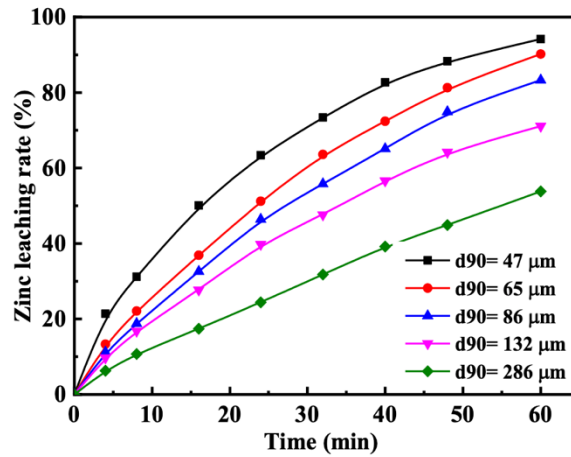


Fig. 7. Effect of particle size on the leaching efficiency of zinc (stirring speed: 450 rpm, temperature: 50 °C, 5-SSA concentration: 0.3 mol/L)

### 3.5. Characterization of zinc metallurgical slag before and after leaching

To investigate the morphology and surface components of zinc metallurgical slag, SEM-EDS analysis of samples before and after leaching was conducted and shown in Fig. 8. As shown in Fig. 8a, the surface of zinc metallurgical slag before leaching was rough, irregular and relatively compact with small particles. Fig. 8b reveals a vast number of well-developed gullies, pores and cracks appeared on the sample surface after the addition of 5-SSA, which could be attributed to the dissolution of zinc oxide. In addition, Fig. 8 also presents that the surface component of zinc metallurgical slag significantly changed after leaching. Specifically, the zinc content was decreased mainly from 38.6% to 0.2%, which further confirmed the successful removal of zinc components from the metallurgical slag surface. In addition, the element contents of Al, K and Cl in samples after leaching were also reduced, which can be attributed to the dissolution of these impurities during the extraction process.

The microstructure features of zinc metallurgical slag before and after leaching were also analyzed and shown in Table 2. As can be seen from it, the BET surface area ( $S_{\text{BET}}$ ) and total volume ( $V_{\text{tot}}$ ) of samples were significantly improved from 7.128 to 15.055  $\text{m}^2/\text{g}$  and 0.006 to 0.010  $\text{cm}^3/\text{g}$ , respectively after leaching. The increase of micropore internal surface area ( $S_{\text{micro}}$ ) and micropore volume ( $V_{\text{micro}}$ ) further confirmed the well-developed micropores and cracks of samples (Ping et al, 2021), which might be assigned to the removal of zinc oxide encapsulated in the sample.

### 3.6. Kinetic analysis

To determine the control step of the leaching rate and to maximize the zinc leaching efficiency, the leach-

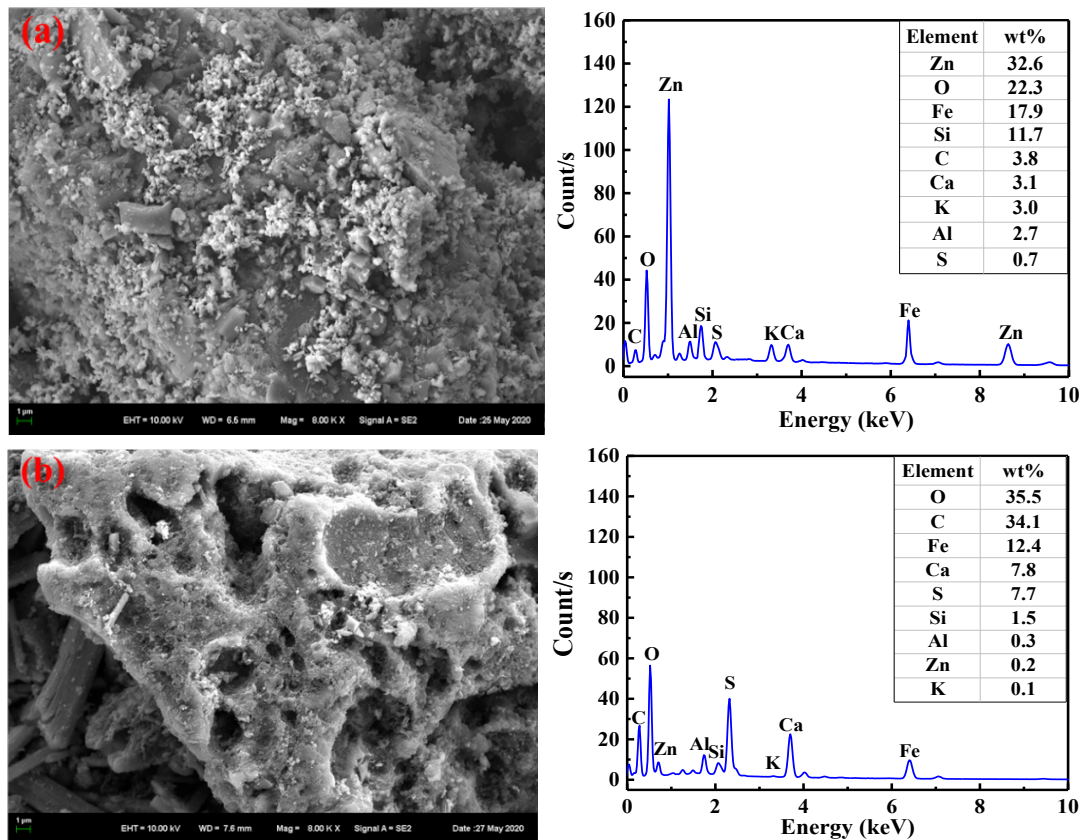


Fig. 8. Morphology and surface components of zinc metallurgical slag (a) before or (b) after leaching with 5-SSA. (leaching conditions: 450 rpm of stirring speed, 50 °C of leaching temperature, 0.300 mol/L of 5-SSA,  $d_{90}=65 \mu\text{m}$  of size fractions)

Table 2. Micro structural features of zinc metallurgical slag before and after leaching

Samples	$S_{\text{BET}}$ (m <sup>2</sup> /g)	$S_{\text{micro}}$ (m <sup>2</sup> /g)	$V_{\text{tot}}$ (cm <sup>3</sup> /g)	$V_{\text{micro}}$ (cm <sup>3</sup> /g)
Before leaching	7.128	3.132	0.006	0.002
After leaching	15.055	8.531	0.010	0.004

ing kinetic model was developed in this study. The chemical reaction of zinc oxide ore in 5-SSA solution is a two-phase reaction system which is usually described by the well-known shrinking-core model (Zhou et al., 2018; Zhu et al., 2019). It was widely applied in some related literature, such as the leaching of malachite, scheelite and uraninite (Behera et al., 2019; Zhu et al., 2019). Thus, the shrinking-core model was selected to depict the leaching kinetics in the present study. The integrated rate equations regarding the surface chemical reactions and product layer diffusion models are defined as Eqs. from 5 to 8 (Luo et al., 2017; Mamo et al., 2019; Mu et al., 2018; Zhou et al., 2018).

$$1 - (1 - x)^{\frac{1}{3}} = kt \quad (5)$$

$$k = mk_s c_0^n / \rho r_0 \quad (6)$$

$$1 - \frac{2}{3}x - (1 - x)^{2/3} = k't \quad (7)$$

$$k't = 2mD_e c_0 / \rho r_0^2 \quad (8)$$

where  $k$  and  $k'$  are the apparent rate constants (min<sup>-1</sup>) for the surface chemical reaction and product layer diffusion respectively;  $x$  is the conversion fraction;  $t$  is the reaction time (s);  $n$  is assumed to be 1;  $m$  is the stoichiometric coefficient in front of ZnO;  $c_0$  is the initial 5-SSA concentration (mol/L);  $D_e$  is the effective diffusivity (m<sup>2</sup>/s);  $\rho$  is the molar density of the raw material (mol/L);  $r_0$  is the initial radius of the solid reactant particle (m);  $k_s$  is the reaction rate constant (m/s).

Table 2. Apparent rate constants and correlation coefficients of two models

Parameter	Product layer diffusion model		Surface chemical reaction model	
	1-2/3x-(1-x) <sup>2/3</sup>		1-(1-x) <sup>1/3</sup>	
	k (min <sup>-1</sup> )	R <sup>2</sup>	k (min <sup>-1</sup> )	R <sup>2</sup>
T/°C				
70	0.0102	0.9820	0.0263	0.9927
60	0.0061	0.9700	0.0167	0.9933
50	0.0031	0.9481	0.0088	0.9911
40	0.0017	0.9575	0.0058	0.9941
30	0.0006	0.8985	0.0035	0.9971
C/(mol/L)				
0.6	0.0042	0.9802	0.0106	0.9952
0.4	0.0035	0.9751	0.0094	0.9956
0.3	0.0031	0.9481	0.0088	0.9991
0.2	0.0025	0.9572	0.0078	0.9984
0.1	0.0018	0.9508	0.0063	0.9991
Stirring speed/rpm				
600	0.0035	0.9776	0.0093	0.9952
450	0.0031	0.9481	0.0088	0.9991
300	0.0026	0.9455	0.0079	0.9994
150	0.0019	0.9529	0.0065	0.9980
Size fraction/μm				
47	0.0038	0.9854	0.0100	0.9935
65	0.0031	0.9481	0.0088	0.9991
86	0.0024	0.9455	0.0074	0.9989
132	0.0015	0.9620	0.0057	0.9956
286	0.0007	0.9224	0.0037	0.9986

According to experimental figures in Figs. 3-6, the surface chemical reaction and product layer diffusion models were investigated and results were shown in Table 2. As is shown, the surface chemical reaction model greatly fits the leaching kinetics with coefficient of determination (R<sup>2</sup>) all exceeded 0.99. On the other hand, most of the R<sup>2</sup> in product layer diffusion model was only ~0.95 or even less. Thus, the surface chemical reaction model was finally adopted in this study to describe the leaching kinetics of zinc metallurgical slag, the results of which were demonstrated in Fig. 9. As can be seen from it, the surface reaction model with equation 1-(1-x)<sup>1/3</sup> exhibited good linear relationships for the zinc leaching rate as a function of stirring speed, leaching temperature, 5-SSA concentration and size fractions. Therefore, the leaching process of zinc oxide in the 5-SSA solution was supposed to be controlled by a surface chemical reaction instead of product layer diffusion.

### 3.7. Activation energy

Activation energy is commonly utilized in leaching kinetic analysis to investigate the control step of the leaching process (Hacarlioglu et al., 2011). The apparent activation energy for the zinc leaching process could be calculated according to the Arrhenius equation by reaction rate constant (*k*) and leaching temperature (*T*) (Ajiboye et al., 2019; Zhu et al., 2019).

$$k = Ae^{-E_a/RT} \quad (9)$$

$$\ln k = \ln A - E_a/RT \quad (10)$$

where *A* is a pre-exponential factor, *R* is the gas constant (8.314 JK<sup>-1</sup>mol<sup>-1</sup>), *E<sub>a</sub>* is the activation energy (kJ/mol). Based on the fore-mentioned equations, the plot of “lnk - 1/T” with the slope of “-*E<sub>a</sub>*/R” was



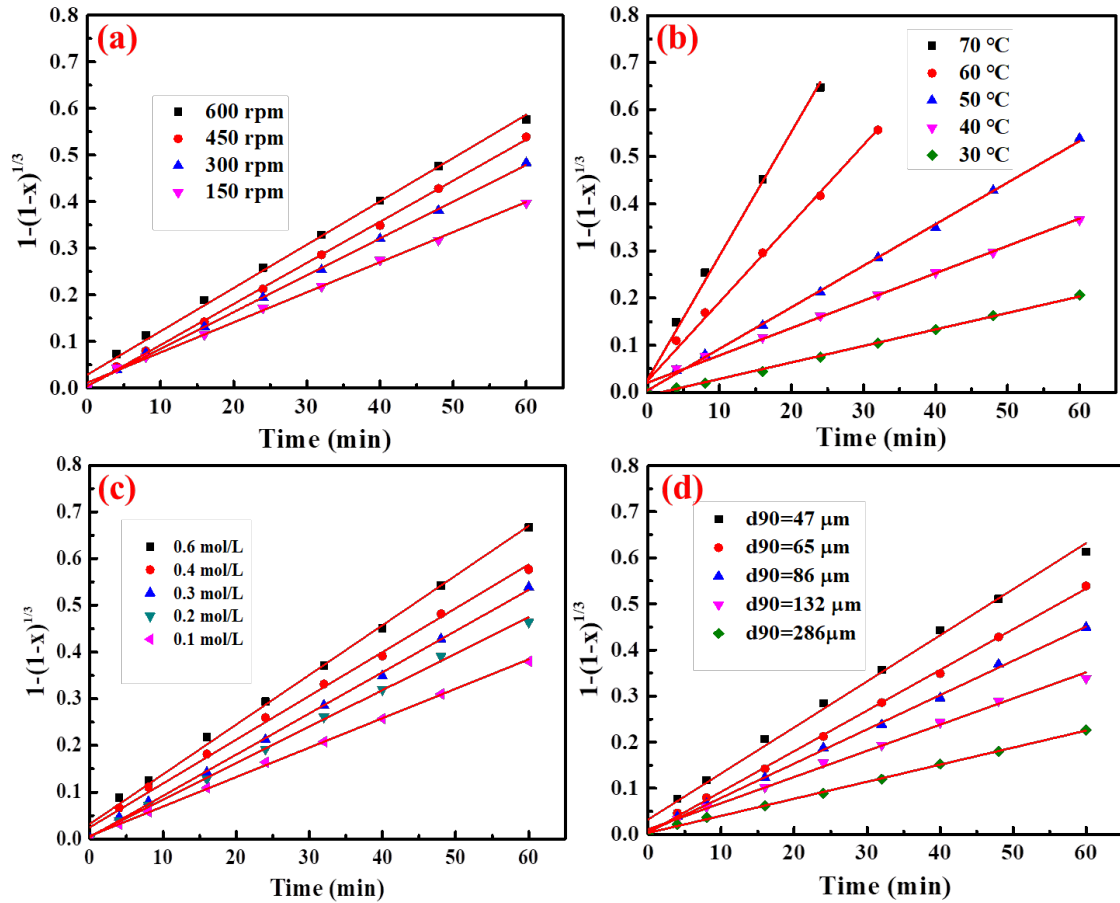


Fig. 9. Surface chemical reaction models as a function of different leaching conditions: (a) stirring speed; (b) leaching temperature; (c) 5-SSA concentration; (d) size fractions

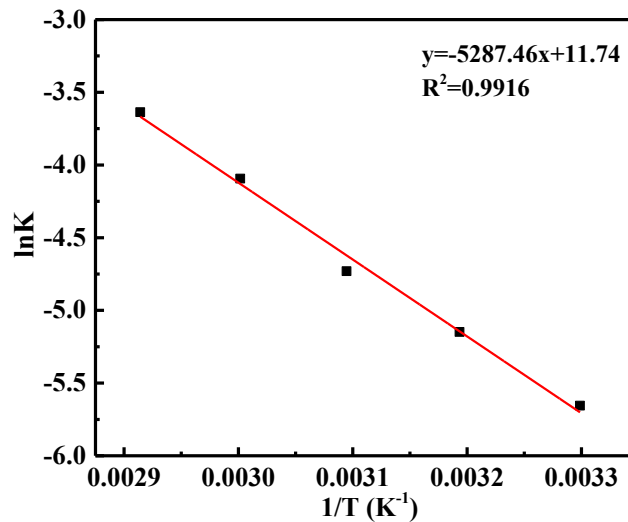


Fig. 10. Curve of  $\ln K$  as a function of  $1/T$

drawn in Fig. 10. The activation energy for the leaching process of zinc metallurgical slag was calculated to be 43.96 kJ/mol. It is widely acknowledged that the activation energy for diffusion-controlled reactions is below 20 kJ/mol while above 40 kJ/mol for the chemical reaction controlled process (Madakkaruppan et al., 2016). Hence, the activation energy analysis further confirmed that the leaching kinetics of zinc metallurgical slag using 5-SSA could be predicted by the surface chemical reaction model.

### 3.8. Establishment of the kinetic equation

To quantitatively describe the influences of stirring speed, leaching temperature, 5-SSA concentration and size fraction on the leaching kinetics of zinc oxide in 5-SSA solution, a semi-empirical equation was put forward and shown as follows (Nie et al., 2020; Zhu et al., 2019):

$$1 - (1 - x)^{\frac{1}{3}} = [K_c \cdot N^a \cdot C^\beta \cdot M^\gamma \cdot e^{-\frac{E_a}{RT}}]t \quad (11)$$

where  $k_c$  is the pre-exponential factor;  $N$ ,  $C$ ,  $M$  and  $T$  stand for the stirring speed (rpm), 5-SSA concentration (mol/L), size fraction ( $\mu\text{m}$ ) and leaching temperature (K), respectively;  $E_a$  is the activation energy;  $R$  is the gas constant. When  $N$  is the only variant while  $C$ ,  $M$  and  $T$  remain constant, Eq. (11) could be simplified as:

$$1 - (1 - x)^{\frac{1}{3}} = K_c \cdot N^a \cdot t \quad (12)$$

$$\frac{d[1-(1-x)^{\frac{1}{3}}]}{dt} = k = K_c \cdot N^a \quad (13)$$

$$\ln \left[ \frac{d[1-(1-x)^{\frac{1}{3}}]}{dt} \right] = \ln k = a \ln N + \ln K_c \quad (14)$$

The curve slope of  $[1-(1-x)^{1/3}]/t$  with different  $N$  corresponded to the reaction rate constant or  $d[1-(1-x)^{1/3}]/dt$ . Thus, the correlation between  $\ln[d[1-(1-x)^{1/3}]/dt]$  and  $\ln N$  was plotted in Fig. 11(a), and the slope of the line was  $a$ , which was calculated to be 0.267. Similarly, the  $\ln[d[1-(1-x)^{1/3}]/dt]$  as a function of  $\ln C$  and  $\ln M$  were also drawn in Figs. 11(b) and 11(c). The slope of which was calculated to be 0.289 and 0.564, respectively. Thus,  $a$ ,  $\beta$  and  $\gamma$  could be substituted by the calculated values and  $k_c=0.035$  could be calculated through the statistical average. Overall, the above semi-empirical equation for the zinc leaching process using 5-SSA can be described as:

$$1 - (1 - x)^{\frac{1}{3}} = [0.035 \cdot N^{0.267} \cdot C^{0.289} \cdot M^{0.564} \cdot e^{-\frac{4023}{T}}]t \quad (15)$$

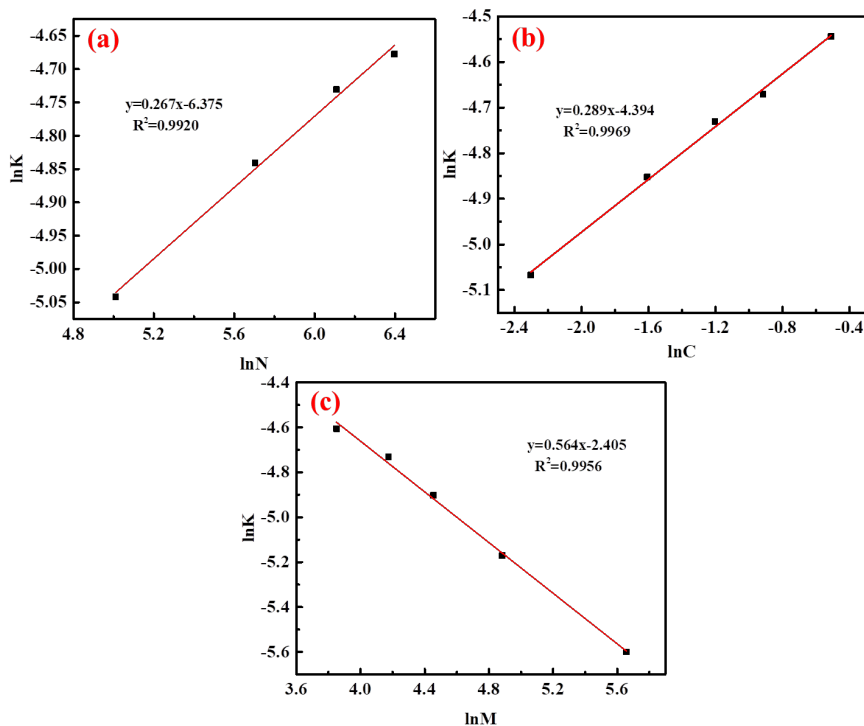


Fig. 11. Curves of  $\ln K$  as a function of different factors: (a) stirring speed; (b) 5-SSA concentration; (c) size fraction

### 4. Conclusions

An organic acid (5-SSA) was utilized as the novel leaching reagent in the leaching process of zinc metallurgical slag. The extraction mechanism mainly depends on the neutral reaction and the

complexation reaction between 5-SSA and zinc oxide. The effects of stirring speed, leaching temperature, 5-SSA concentration, and size fraction on the leaching behavior of zinc metallurgical slag were also investigated. A zinc leaching efficiency of 94.2% was achieved under the appropriate leaching conditions (450 rpm of stirring speed, 50 °C of leaching temperature, 0.3 mol/L of 5-SSA concentration, and  $d_{90}=65 \mu\text{m}$  of size fraction), indicating that 5-SSA was an excellent leaching reagent for the zinc oxide. Further explorations showed that a vast number of well-developed gullies, pores, and cracks appeared on the sample surface after the addition of 5-SSA, which could be attributed to the dissolution of zinc oxide. The zinc leaching rate of metallurgical slag in the 5-SSA solution fitted well with the shrinking-core kinetic model with the surface chemical reaction as the control step. The apparent activation energy was calculated to be 33.45 kJ/mol. The semi-empirical equation was eventually established for the zinc leaching process using 5-SSA.

### Acknowledgments

The authors gratefully thank the National Natural Science Foundation of China (51904106, 51904214), Natural Science Foundation of Hebei Province (E2019209494), Science and Technology Project of Tangshan (19130218g), Natural Science Foundation of Hebei Province (E2018209085) for their financial support, Open Foundation of Hubei Key Laboratory for Efficient Utilization and Agglomeration of Metallurgic Minerals Resources (2019zy010) and the Fundamental Research Funds for the Central Universities (WUT:203208004).

### References

- AJIBOYE, E.A., PANDA, P.K., ADEBAYO, A.O., AJAYI, O.O., TRIPATHY, B.C., GHOSH, M.K., BASU, S., 2019. *Leaching kinetics of Cu, Ni and Zn from waste silica rich integrated circuits using mild nitric acid*, 188, 161-168.
- ASADI, T., AZIZI, A., LEE, J.C., JAHANI, M., 2017. *Leaching of zinc from a lead-zinc flotation tailing sample using ferric sulphate and sulfuric acid media*. *Journal of Environmental Chemical Engineering*, 5(5), 4769-4775.
- BEHERA, S.S., PANDA, S.K., MANDAL, D., PARHI, P.K., 2019. *Ultrasound and Microwave assisted leaching of neodymium from waste magnet using organic solvent*. *Hydrometallurgy*, 185, 61-70.
- BEHNAJADY, B., MOGHADDAM, J., 2017. *Selective leaching of zinc from hazardous As-bearing zinc plant purification filter cake*. *Chemical Engineering Research and Design*, 117, 564-574.
- BRYNDAL, I., LEDOUX-RAK, I., LIS, T., RATAJCZAK, H., 2014. *Search for molecular crystals with NLO properties: 5-Sulfosalicylic acid with nicotinamide and isonicotinamide*. *Journal of Molecular Structure*, 1068, 77-83.
- CAO, Y., YAN, L., HUANG, H., DENG, B., 2016. *Selenium speciation in radix puerariae using ultrasonic assisted extraction combined with reversed phase high performance liquid chromatography-inductively coupled plasma-mass spectrometry after magnetic solid-phase extraction with 5-sulfosalicylic acid functionalized magnetic nanoparticles*. *Spectrochimica Acta Part B: Atomic Spectroscopy*, 122, 172-177.
- CHAIRAKSA-FUJIMOTO, R., MARUYAMA, K., MIKI, T., NAGASAKA, T., 2016. *The selective alkaline leaching of zinc oxide from Electric Arc Furnace dust pre-treated with calcium oxide*. *Hydrometallurgy*, 159, 120-125.
- CHEN, C., ZHU, X., WU, Y., SUN, H., ZHANG, G., ZHANG, W., GAO, Z., 2014. *5-Sulfosalicylic acid catalyzed direct Mannich reaction in pure water*. *Journal of Molecular Catalysis A: Chemical*, 395, 124-127.
- EHSANI, Í., OBUT, A., 2019. *Conversion behaviours of Sr- and Ca-containing solids in dissolved carbonate containing alkaline pregnant zinc leaching solutions*. *Minerals Engineering*, 135, 9-12.
- FALAGÁN, C., YUSTA, I., SÁNCHEZ-ESPAÑA, J., JOHNSON, D.B., 2017. *Biologically-induced precipitation of aluminium in synthetic acid mine water*. *Minerals Engineering*, 106, 79-85.
- GU, K., LI, W., HAN, J., LIU, W., QIN, W., CAI, L., 2019. *Arsenic removal from lead-zinc smelter ash by NaOH-H<sub>2</sub>O<sub>2</sub> leaching*. *Separation and Purification Technology*, 209, 128-135.
- GÜLER, E., SEYRANKAYA, A., 2016. *Precipitation of impurity ions from zinc leach solutions with high iron contents - A special emphasis on cobalt precipitation*. *Hydrometallurgy*, 164, 118-124.
- HACARLIOGLU, P., ACHENIE, L., TED OYAMA, S., 2011. *Ab Initio Studies of Silica-Based Membranes*, In *Inorganic Polymeric and Composite Membranes - Structure, Function and Other Correlations*, pp. 79-90.
- IRANNAJAD, M., MESHKINI, M., AZADMEHR, A.R., 2013. *Leaching of zinc from low grade oxide ore using organic acid*. *Physicochemical Problems of Mineral Processing*, 49(2), 547-555.
- JIN, Y., ZENG, C., LÜ, Q.-F., YU, Y., 2019. *Efficient adsorption of methylene blue and lead ions in aqueous solutions by 5-sulfosalicylic acid modified lignin*. *International Journal of Biological Macromolecules*, 123, 50-58.

- LI, J., GAO, Y., GAO, Y., CHEN, Z., WANG, R., XU, Z., 2020. *Study on aluminum removal through 5-sulfosalicylic acid targeting complexing and D290 resin adsorption*. Minerals Engineering, 147, 106175.
- LI, Y., LIU, H., PENG, B., MIN, X., HU, M., PENG, N., YUANG, Y., LEI, J., 2015. *Study on separating of zinc and iron from zinc leaching residues by roasting with ammonium sulphate*. Hydrometallurgy, 158, 42-48.
- LIN, H.B., LIAO, Z.Q., DAI, Y.H., WANG, Y.Y., GUO, H.X., 2018. *Design of multiple efficient molecular logic devices based on molecular systems containing bovine serum albumin and 5-sulfosalicylic acid*. Sensors and Actuators B: Chemical, 273, 672-680.
- LIU, C., ZHENG, Y.F., YANG, S.Y., FU, W., CHEN, X., 2021. *Exploration of a novel depressant polyepoxysuccinic acid for the flotation separation of pentlandite from lizardite slimes*. Applied Clay Science, 202, 105939.
- LIU, X., WANG, J., GHENI, A., ELGAWADY, M.A., 2018. *Reduced zinc leaching from scrap tire during pavement applications*. Waste Management, 81, 53-60.
- LUO, M.-J., LIU, C.-L., XUE, J., LI, P., YU, J.-G., 2017. *Leaching kinetics and mechanism of alunite from alunite tailings in highly concentrated KOH solution*. Hydrometallurgy, 174, 10-20.
- MADAKKARUPPAN, V., PIUS, A., T, S., GIRI, N., SARBAJNA, C., 2016. *Influence of microwaves on the leaching kinetics of uraninite from a low grade ore in dilute sulfuric acid*. J. Hazard. Mater., 313, 9-17.
- MAHEDI, M., CETIN, B., DAYIOGLU, A.Y., 2019. *Leaching behavior of aluminum, copper, iron and zinc from cement activated fly ash and slag stabilized soils*. Waste Management, 95, 334-355.
- Mamo, S.K., Elie, M., Baron, M.G., Simons, A.M., GONZALEZ-RODRIGUEZ, J., 2019. *Leaching kinetics, separation, and recovery of rhenium and component metals from CMSX-4 superalloys using hydrometallurgical processes*. Separation and Purification Technology, 212, 150-160.
- MU, W.N., LU, X.Y., CUI, F.H., LUO, S.H., ZHAI, Y.C., 2018. *Transformation and leaching kinetics of silicon from low-grade nickel laterite ore by pre-roasting and alkaline leaching process*. Transactions of Nonferrous Metals Society of China, 28(1), 169-176.
- NIE, W., WEN, S., FENG, Q., LIU, D., ZHOU, Y., 2020. *Mechanism and kinetics study of sulfuric acid leaching of titanium from titanium-bearing electric furnace slag*. Journal of Materials Research and Technology, 9(2), 1750-1758.
- PING, A., XIA, W.C., PENG, Y.L., XIE, G.Y., 2021. *Comparative filtration and dewatering behavior of vitrinite and inertinite of bituminous coal: Experiment and simulation study*. International Journal of Mining Science and Technology, 31(2), 233-240.
- RAO, S., YANG, T., ZHANG, D., LIU, W., CHEN, L., HAO, Z., XIAO, Q., WEN, J., 2015. *Leaching of low grade zinc oxide ores in NH<sub>4</sub>Cl-NH<sub>3</sub> solutions with nitrilotriacetic acid as complexing agents*. Hydrometallurgy, 158, 101-106.
- RU, Z.G., PAN, C.X., LIU, G.H., WANG, X.T., DOU, G.Y., ZHU, K.S., 2015. *Leaching and recovery of zinc from leaching residue of zinc calcine based on membrane filter press*. Transactions of Nonferrous Metals Society of China, 25(2), 622-627.
- ŞAHİN, M., ERDEM, M., 2015. *Cleaning of high lead-bearing zinc leaching residue by recovery of lead with alkaline leaching*. Hydrometallurgy, 153, 170-178.
- SEYED GHASEMI, S.M., AZIZI, A., 2018. *Alkaline leaching of lead and zinc by sodium hydroxide: kinetics modeling*. Journal of Materials Research and Technology, 7(2), 118-125.
- WANG, L., SONG, S., GAO, H., WANG, L., YANG, S., LIU, C., 2020a, *The optimization and characterization of the recycling utilization of raffinate in the copper leaching process*. Journal of Materials Research and Technology, 9(2), 2214-2222.
- WANG, W., TANG, B., WU, S., GAO, Z., JU, B., TENG, X., ZHANG, S., 2017. *Controllable 5-sulfosalicylic acid assisted solvothermal synthesis of monodispersed superparamagnetic Fe<sub>3</sub>O<sub>4</sub> nanoclusters with tunable size*. Journal of Magnetism and Magnetic Materials, 423, 111-117.
- WANG, Y., LI, J., GAO, Y., YANG, Y., GAO, Y., XU, Z., 2020b, *Removal of aluminum from rare-earth leaching solutions via a complexation-precipitation process*. Hydrometallurgy, 191, 105220.
- XIAO, G., WEN, R., WEI, D., 2016. *Effects of the hydrophobicity of adsorbate on the adsorption of salicylic acid and 5-sulfosalicylic acid onto the hydrophobic-hydrophilic macroporous polydivinylbenzene/polymethylacrylethyl-enediamine IPN*. Fluid Phase Equilibria, 421, 33-38.
- XU, T.Y., WANG, H., LI, J.M., ZHAO, Y.L., HAN, Y.H., WANG, X.L., HE, K.-H., WANG, A.-R., SHI, Z.-F., 2019. *A water-stable luminescent Zn(II) coordination polymer based on 5-sulfosalicylic acid and 1,4-bis(1H-imidazol-1-yl)benzene for highly sensitive and selective sensing of Fe<sup>3+</sup> ion*. Inorganica Chimica Acta, 493, 72-80.
- YANG, S., LI, C., WANG, L., 2017. *Dissolution of starch and its role in the flotation separation of quartz from hematite*. Powder Technology, 320, 346-357.

- YANG, S., LI, H., SUN, Y., CHEN, Y., TANG, C., HE, J., 2016a. *Leaching kinetics of zinc silicate in ammonium chloride solution*. Transactions of Nonferrous Metals Society of China, 26(6), 1688-1695.
- YANG, T., RAO, S., ZHANG, D., WEN, J., LIU, W., CHEN, L., ZHANG, X., 2016b. *Leaching of low grade zinc oxide ores in nitrilotriacetic acid solutions*. Hydrometallurgy, 161, 107-111.
- ZHANG, C., MIN, X., ZHANG, J., WANG, M., LI, Y., FEI, J., 2016a. *Reductive clean leaching process of cadmium from hydrometallurgical zinc neutral leaching residue using sulfur dioxide*. Journal of Cleaner Production, 113, 910-918.
- ZHANG, Y., HUA, Y., GAO, X., XU, C., LI, J., LI, Y., ZHANG, Q., XIONG, L., SU, Z., WANG, M., RU, J., 2016b. *Recovery of zinc from a low-grade zinc oxide ore with high silicon by sulfuric acid curing and water leaching*. Hydrometallurgy, 166, 16-21.
- ZHOU, X., CHEN, Y., YIN, J., XIA, W., YUAN, X., XIANG, X., 2018. *Leaching kinetics of cobalt from the scraps of spent aerospace magnetic materials*. Waste Management, 76, 663-670.
- ZHU, X., LIU, X., ZHAO, Z., 2019. *Leaching kinetics of scheelite with sodium phytate*. Hydrometallurgy, 186, 83-90.